

## Durham Research Online

---

### Deposited in DRO:

12 December 2016

### Version of attached file:

Accepted Version

### Peer-review status of attached file:

Peer-reviewed

### Citation for published item:

Lee, Rachael and Mason, Sax A. and Mossou, Estelle and Lamming, Glenn and Probert, Michael R. and Steed, Jonathan W. (2016) 'Neutron diffraction studies on guest-induced distortions in urea inclusion compounds.', *Crystal growth design*, 16 (12). pp. 7175-7185.

### Further information on publisher's website:

<https://doi.org/10.1021/acs.cgd.6b01371>

### Publisher's copyright statement:

This document is the Accepted Manuscript version of a Published Work that appeared in final form in *Crystal Growth Design*, copyright © American Chemical Society after peer review and technical editing by the publisher. To access the final edited and published work see <https://doi.org/10.1021/acs.cgd.6b01371>.

### Additional information:

---

### Use policy

The full-text may be used and/or reproduced, and given to third parties in any format or medium, without prior permission or charge, for personal research or study, educational, or not-for-profit purposes provided that:

- a full bibliographic reference is made to the original source
- a [link](#) is made to the metadata record in DRO
- the full-text is not changed in any way

The full-text must not be sold in any format or medium without the formal permission of the copyright holders.

Please consult the [full DRO policy](#) for further details.

# Neutron Diffraction Studies on Guest-Induced Distortions in Urea Inclusion Compounds

*Rachael Lee,<sup>a,b</sup> Sax A. Mason,<sup>c</sup> Estelle Mossou,<sup>c</sup> Glenn Lamming,<sup>b</sup> Michael R. Probert<sup>b</sup> and Jonathan W. Steed<sup>a\*</sup>*

<sup>a</sup> Department of Chemistry, Durham University, South Road, Durham, DH1 3LE, UK.

<sup>b</sup> School of Chemistry, Newcastle University, Newcastle-Upon-Tyne, NE1 7RU, UK.

<sup>c</sup> Institut Laue-Langevin, BP 156, 38042 Grenoble, Cedex 9, France

## Abstract

Single crystal neutron structures at several temperatures have been determined for  $\beta$ -phase urea inclusion compounds containing hexadecane, 1,6-dibromohexane and 2,7-octanedione guests. The neutron structure of the ‘partial channel’ co-crystal of urea and DMF is also reported. Here we present an in-depth discussion and analysis of the structure and bonding of this urea series, in particular, how the guest compound affects the symmetry and hydrogen bonding of the host urea network. Additionally, we address the challenge of obtaining crystals suitable for neutron diffraction and present a new heating/cooling device to aid crystallisation.

## Introduction

Urea inclusion compounds (UICs), the  $\beta$ -phase of urea, were first discovered in 1949 by Schlenk and described as “urea addition crystals”.<sup>1</sup> Since then this class of compound has

been studied comprehensively, and found to display various structural and behavioral characteristics of interest, largely influenced by the nature of the guest molecule. These crystals have a hexagonally symmetrical honeycomb channel structure formed by an extensively hydrogen bonded helical urea network which encapsulates the guest molecules.<sup>2</sup> A variety of guest compounds facilitate UIC formation, within certain limitations; typically relatively long chain molecules with little or no branching. This includes long chain alkanes  $C_7H_{16}$  to  $C_{20}H_{42}$ ,<sup>3</sup>  $\alpha,\omega$ -dihaloalkanes  $X(CH_2)_n X$  where  $n = 7-10$ ,<sup>4</sup> and  $(\alpha+1),(\omega-1)$ -diketones,<sup>5</sup> among other long chain and slightly branched compounds. When the guest is altered, so too is the behavior of the host network. Despite the degree of interest in this class of compounds, few neutron diffraction experiments have been used in their study, and then only on incommensurate examples.<sup>6</sup> Neutron Laue diffraction had been utilized to study phase transitions of an *n*-nonadecane UIC, identifying a previously unseen phase transition and associated superspace group.<sup>7</sup> *n*-Hexadecane/urea has been previously studied by both X-ray and neutron diffraction techniques but no atomic coordinates are reported in the CSD.<sup>6,8</sup>

Here we report the first commensurate urea inclusion compound structures elucidated from single crystal neutron diffraction experiments.

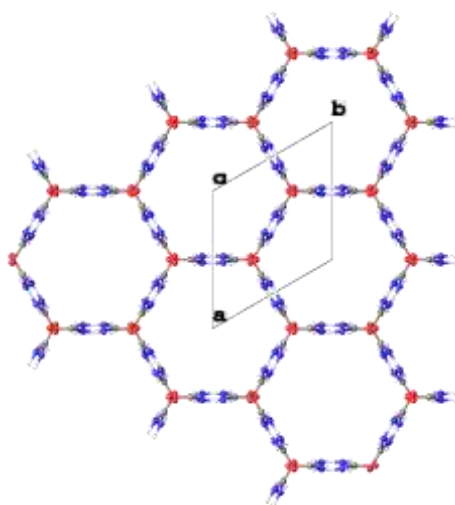


Figure 1. X-ray structure of urea with hexadecane guest, viewed down  $c$  axis. Host structure only is shown for clarity.

The host-guest relationship is classed as incommensurate when no sensible integers can be found to satisfy the relationship  $nc_g = mc_h$ , where  $c_h$  and  $c_g$  are the repeat distances of the host and guest, respectively.<sup>9</sup> The dynamic disorder of the guest causes the overall structure to maintain the hexagonal symmetry of the urea network. The simplest class of UIC contains an alkane guest, which has an incommensurate host-guest relationship and significant disorder in the host channels.<sup>3</sup>

A commensurate relationship between the host and guest may also be observed, in cases where hydrogen bonding occurs between the guest and urea molecules, or when the guest can adopt a conformation which is complementary to the periodicity of the host. A number of bis(methyl) ketone UICs, display a commensurate relationship as the carbonyl groups form hydrogen bonds with adjacent urea molecules in the host wall.<sup>5</sup> In the case of 2,10-undecanedione/urea, the resulting distortion creates macroscopic domains within the crystal structure which are susceptible to reorientation when a small compressive stress is applied to certain crystal faces, resulting in ferroelastic behavior.<sup>10</sup>

UICS of 1,6-dibromohexane, 1-bromo-6-chlorohexane and 1,6-dichlorohexane also exhibit a commensurate host-guest relationship.<sup>4</sup> In this instance the guest coils into an atypical gauche conformation to avoid unfavorable guest-guest interactions and creates a distortion of the host network away from hexagonal symmetry as a result of the cross sectional shape of the dihaloalkane.<sup>4, 11</sup> The guests undergo torsional conversions between gauche conformations in a temperature dependent manner; at higher temperatures the guests are more mobile and the structures experience a phase transition to a higher symmetry hexagonal

phase, as increased frequency of torsional jumps equilibrates the internal stress applied to the host by the guest.

Temperature dependent phase transitions are consistently seen across a range of UICs, for example both 1,10-dibromodecane and 1,12-dibromododecane UICs display a single-crystal to single-crystal phase transition going from a high temperature hexagonal phase typical of high symmetry UICs, to a lower temperature orthorhombic structure.<sup>12</sup> In both cases, this host/guest relationship remains incommensurate, much like that of alkane UICs. This further highlights the importance of guest size on commensurability of UICs, as 1,6-dibromohexane from the same  $\alpha,\omega$ -dihaloalkane family of compounds has a commensurate relationship with the urea network.

The UIC of 2-bromotetradecane also transitions from a high temperature hexagonal phase to a lower temperature orthorhombic phase, and further to a monoclinic phase below 142 K.<sup>13</sup> The distortions of the channel on lowering the temperature can be attributed to changes in guest molecule orientation, although the structure is incommensurate regardless of temperature. As the guests' dynamic orientational disorder is reduced at lower temperature, the host network adopts a lower symmetry, accommodating the change.

In this work we undertake a detailed study of the hydrogen bonding interactions in the urea host network and between urea and guest molecules using complementary single crystal X-ray and neutron diffraction. Particular emphasis is placed on examples of UICs which, due to unusual interaction between the host and guest, display atypical structural features resulting in distortion of the host network away from the classical hexagonal symmetry of  $\beta$ -urea.<sup>5, 11</sup>

## Experimental

1,6-Dibromohexane, hexadecane and urea were obtained from Sigma-Aldrich. DMF was obtained from Fisher Scientific. 2,7-Octanedione was obtained from Aurora Fine Chemicals LLC. 1,6-Dibromohexane/urea (DBH) was crystallized by slow cooling from MeOH. Urea-

DMF (UDM) was crystallized from a concentrated solution of urea in DMF.<sup>14</sup> Hexadecane UIC (HEX) was crystallized by adding liquid hexadecane to a solution of urea in MeOH, then adding 2-propanol dropwise until the components were miscible. The solution was agitated by sonication until clear and allowed to slowly evaporate.

Single crystal X-ray data were collected on an Agilent Gemini S-Ultra diffractometer equipped with Cryostream (Oxford Cryosystems) open-flow nitrogen cryostat, using graphite monochromated Mo K $\alpha$ -radiation ( $\lambda = 0.71069\text{\AA}$ ). All structures were solved by direct methods and refined by full-matrix least squares on  $F^2$  for all data using SHELX-2015/2<sup>15</sup> and OLEX2<sup>16</sup> software. All non-hydrogen atoms were refined with anisotropic displacement parameters, H-atoms were located on the difference Fourier maps and refined isotropically. All X-ray structures henceforth discussed refer to those reported in existing literature,<sup>5, 8, 11, 14</sup> except for HEX, which was re-determined in order to obtain atomic coordinates of the host network.

Neutron data were collected on the thermal four-circle D19 diffractometer at ILL, Grenoble which uses a large position sensitive detector ( $120^\circ \times 30^\circ$ ) and two stage Displex cryorefrigerator for cooling. An incident wavelength of  $1.1698\text{ \AA}$  was used for DBH and HEX, and UDM. For OCT a wavelength of  $1.4547\text{ \AA}$  was used.

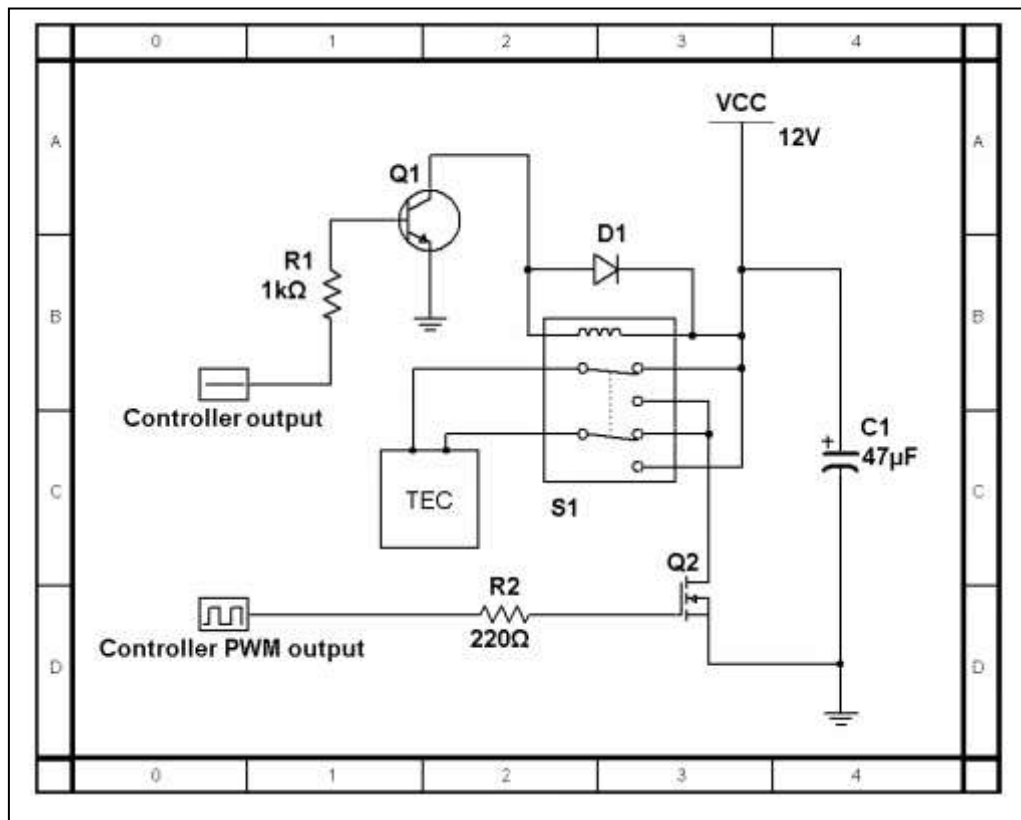
High pressure studies were carried out using a diamond anvil cell, by loading crystals of each compound into a gasket of 0.25 mm steel pre-indented to 0.15 mm with a precision drilled  $300\text{ }\mu\text{m}$  hole, situated between two diamond anvils.<sup>17</sup> Paraffin oil was used as the hydrostatic medium and a ruby chip was added to the cell to allow pressure determination by the ruby fluorescence method.<sup>18</sup> Data were collected on the XIPHOS II diffractometer at Newcastle University, using a four-circle Huber goniometer with Ag-K $\alpha$   $I\mu S$  generator.<sup>19-21</sup>

Urea / 2,7-octanedione (OCT) was crystallized using a specially designed Peltier thermoelectric cooling (TEC) unit (see below). A concentrated methanol solution of urea and

2,7-octanedione was cooled from 50°C to 12°C over a period of 4 days and held at 12°C for a further 2 days to optimize crystal size. After this point, the crystals proved to degrade rapidly unless removed from the mother liquor and stored under inert oil.

### Design of a heating/cooling Peltier thermoelectric cooler

Schematic 1 shows the circuit design on the Peltier TEC control unit. The controller outputs are 5V TTL logic level, all resistors are rated for ¼ watt and the TEC used was a TEC1-12706 (72 W). The relay S1 is a double-pole double-throw type wired in an H-bridge configuration. By altering the frequency of the pulse-width modulated signal supplied to the gate of the N-channel MOSFET Q2 (P35NF10), the power delivered to the TEC is governed by the controller. The direction that heat is pumped across the TEC can be changed by signaling the NPN transistor Q1 (2N3904), this causes the relay S1 to latch and inverts the polarity applied across the TEC. Source code for the controller and additional information on the circuit design can be found at: <https://github.com/nu-xtal-tools/ControlTEC>.



Schematic 1. Circuit design of the Peltier TEC control unit

## Results

Urea inclusion compounds of hexadecane, 2,7-octanedione, 1,6-dibromohexane and N,N-dimethylformamide (Figure 2), were crystallized and analyzed by both X-ray and neutron diffraction at a range of temperatures. These particular examples were chosen as they represent a series where the changing guest,<sup>4, 5, 8</sup> or co-former,<sup>14</sup> varies the symmetry and bonding in a pseudo-systematic way. HEX is a representative example of a ‘typical’ hexagonal urea clathrate and is the simplest and most symmetrical UIC in the group, OCT maintains hexagonal symmetry at the expense of hydrogen bonding continuity and unit cell size, DBH has monoclinic symmetry as a result of internal stress applied by a bulky guest molecule, and UDM is not a traditional channel type inclusion compound, but maintains certain structural features similar to the hexagonal channel along one axis. In addition, the guest molecules were chosen for OCT and DBH as their UIC structures were known to be commensurate, eliminating any barriers to observing the finer detail of hydrogen bonding, which is difficult to resolve in incommensurate structures due to guest disorder.

Here we outline the main features of each structure. Further analysis and comparison of structure and bonding can be found in the discussion section.



Table 1. Summary of crystallographic data from neutron diffraction experiments.

	HEX		DBH			OCT	UDM	
Formula	$\text{C}_9\text{H}_{12}\text{N}_6\text{O}_3$		$\text{C}_6\text{H}_{12}\text{Br}_2 6(\text{CH}_4\text{N}_2\text{O})$			$\text{C}_8\text{H}_{14}\text{O}_2 7(\text{CH}_4\text{N}_2\text{O})$	$\text{C}_3\text{H}_4\text{NO} 3(\text{CH}_4\text{N}_2\text{O})$	
$T/ \text{K}$	150	260	30	120	260	30	30	120
Crystal system	Hexagonal		Monoclinic			Hexagonal	Triclinic	
Space group	$P6_522$		$P2_1/n$			$P6_522$	$P\bar{1}$	
$a/ \text{\AA}$	8.1529(5)	8.1219(14)	8.5518(2)	8.5793(6)	8.5793(6)	8.1007(5)	7.3797(2)	7.4648(3)
$b/ \text{\AA}$	8.1529(5)	8.1219(14)	10.8605(2)	10.8922(8)	10.8922(8)	8.1007(5)	9.9588(3)	9.8804(4)
$c/ \text{\AA}$	10.9819(6)	10.9891(13)	13.3296(3)	13.4160(12)	13.4160(12)	76.213(5)	10.9509(2)	10.8588(3)
$\alpha / ^\circ$	90		90			90	64.5386(13)	65.2370(19)
$\beta / ^\circ$	90		92.919(2)	92.779(7)	92.779(7)	90	77.4999(14)	78.769(2)
$\gamma / ^\circ$	90		90			90	67.8699(14)	69.732(2)
$Z$	2		2			6	4	
$Z'$	0.167		0.5			0.5	2	
$Z''$	2		4			5	4	
$V/ \text{\AA}^3$	632.17(7)	627.78(17)	1236.40(5)	1252.22(17)	1252.2(2)	4331.1(5)	671.68(3)	681.06(5)
$D_c$	1.325	1.335	1.623	1.603	1.603	1.294	1.253	1.235
Unique relfns.	2838	2453	12134	13110	13186	18067	7491	7193
Completeness %	93	90	92	92	92	97	88	88
$R_1$	0.068	0.062	0.032	0.042	0.043	0.091	0.055	0.054
$wR_2$	0.188	0.181	0.066	0.093	0.088	0.203	0.142	0.014
GooF	1.12	1.11	1.19	1.16	1.05	1.15	1.17	1.11

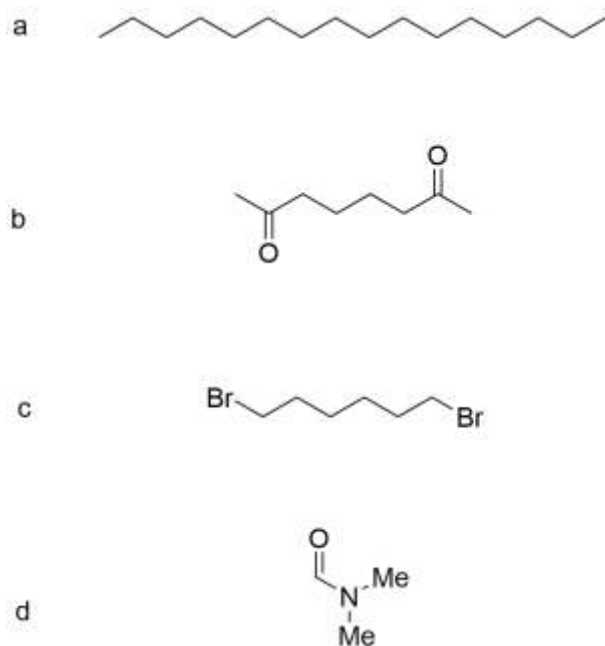


Figure 2. a) Hexadecane. a) 2,7-octanedione. c) 1,6-dibromohexane. d) N,N-dimethylformamide.

### Urea Hexadecane

The X-ray crystal structure of urea/hexadecane, was reported by Chatani *et al.* in 1976.<sup>8</sup> Figure 3, derived from the re-determined X-ray structure, demonstrates how the complex displays a characteristic hexagonal channel motif, with the 16 carbon atom guest molecule hexadecane occupying the channels.<sup>22</sup> Given the lack of hydrogen bonding capability or other functionality in the included hydrocarbon, the guest has an incommensurate relationship with the host network and is significantly disordered throughout the structure. It appears in the X-ray experiment as a ‘smear’ of electron density within the one dimensional channels. This structure offers a useful example of a symmetrical channel essentially unperturbed by guest interactions given the  $\beta_0$  hexagonal framework has never been crystallized without a guest present.<sup>23</sup>

The structure and dimensions of this UIC represent a model urea framework against which other analogues can be compared. This contrast will contribute to understanding the extent to which the guest can influence the nature of the host network.

---

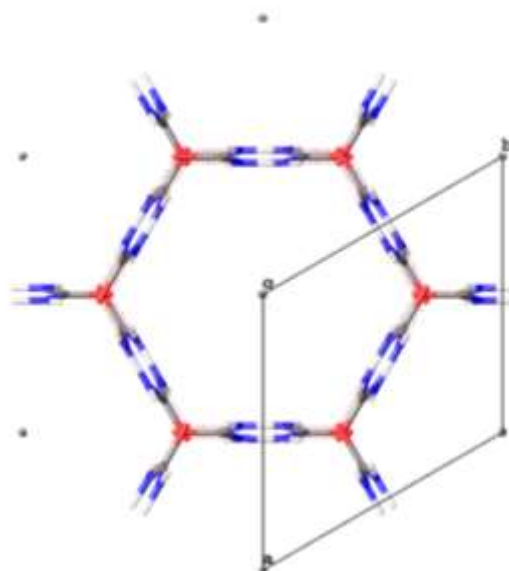


Figure 3. View along  $c$  axis of urea/hexadecane showing cross section of one 1D channel with unit cell superimposed. Hexadecane appears as a grey dot in the channel center.

At 150 K the UIC of hexadecane adopts space group  $P6_122$  (Table 1). Below 150 K, a phase transition is observed which consistently causes the crystals to become multiply twinned and makes further single crystal diffraction unfeasible. Yeo *et al.* determined this low temperature phase to be orthorhombic  $P2_12_12_1$  from powder diffraction data by Rietveld refinement, using the high temperature phase as a model, producing a distorted form of the hexagonal phase arising from reduced motion of the guest in the channels.<sup>24</sup> When the crystal (Figure 4) was warmed back to 151 K, the phase transition is reversible, and the split peaks re-merge (Figure 5). This is notable as typically, split diffraction spots are associated with degradation and cracking of the crystal due to a phase transition or other effect, and often is not reversible.



Figure 4. Crystal of HEX mounted on a vanadium pin.

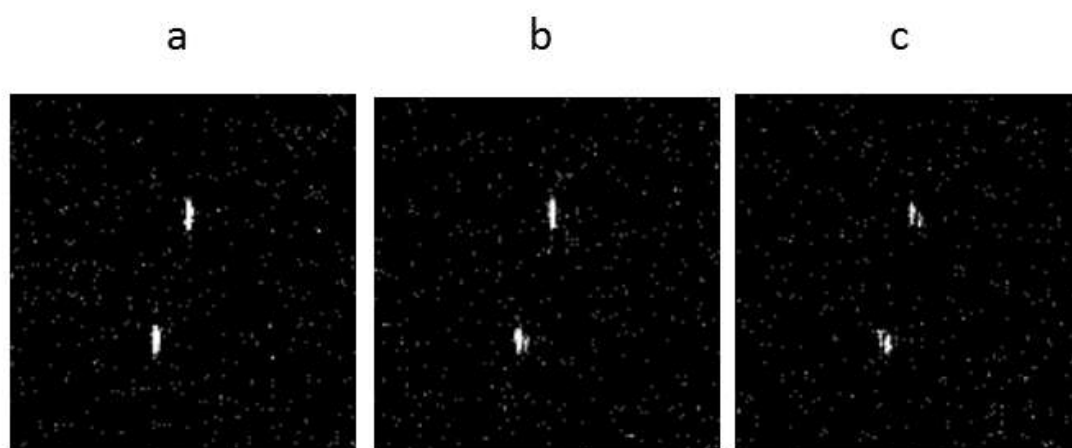


Figure 5. Peak splitting on cooling HEX a) 151 K, b) 150 K, c) 149 K.

A similar example of such unusual behavior is seen for piroxicam monohydrate,<sup>25</sup> which on cooling between 120 and 22 K undergoes peak splitting. Within 11 hours, the peaks have re-merged although in this case, there is no evidence for a first order phase transition as both the 120 K data and that collected at 22 K after peak coalescence show the same monohydrate phase and the re-merging of the peaks is time dependent, rather than temperature dependent.

The asymmetric unit of HEX contains a partial urea molecule, thus the hydrogen bonding for the entire system can be described by the two symmetry unique hydrogen bonds of the

NH<sub>2</sub> group (Figure 6). Data collected by single crystal neutron diffraction were used to determine the hydrogen bonding distances between urea molecules, detailed in Table 4.

---

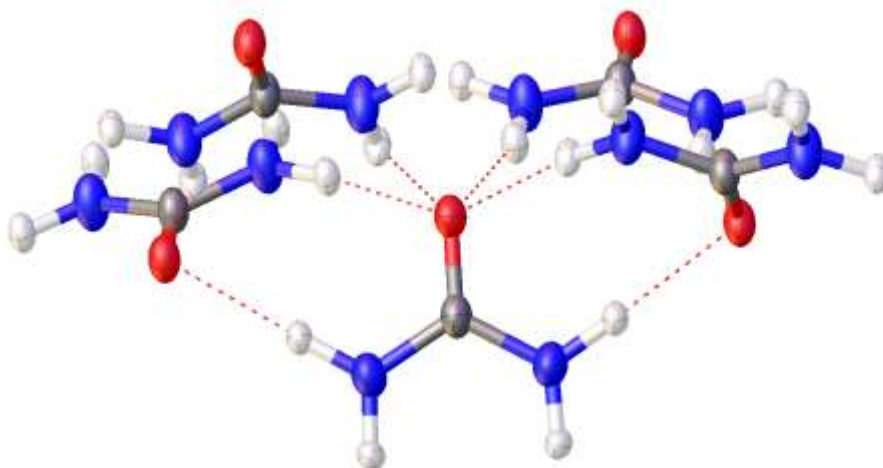


Figure 6. Hydrogen bonds in UIC of hexadecane. All urea molecules are equivalent. Hexadecane guest omitted for clarity.

## Urea 1,6-dibromohexane

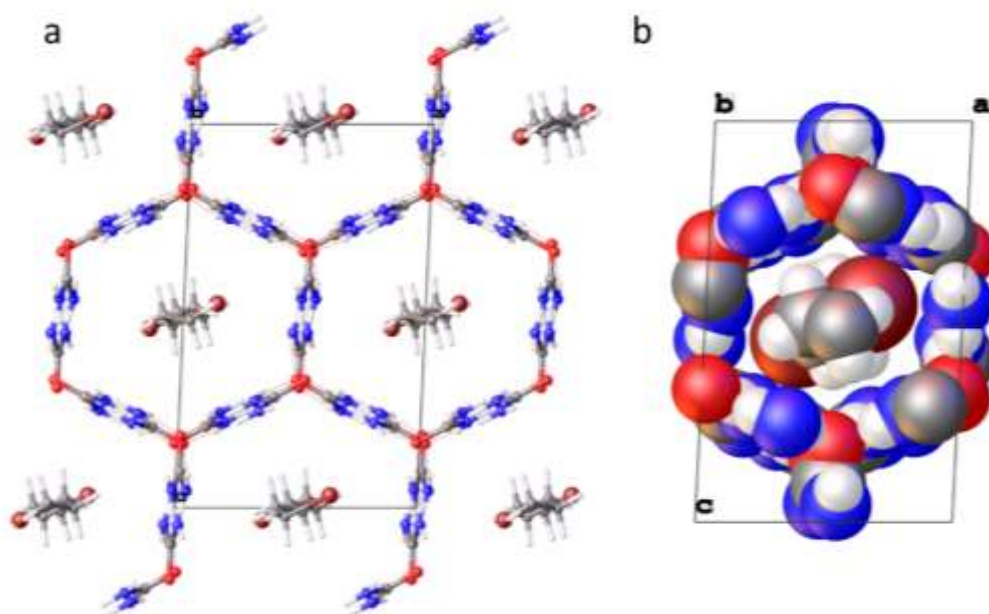


Figure 7. a) View down the *b* axis of 1,6-dibromohexane UIC with unit cell superimposed. b) Space filling representation of the unit cell.

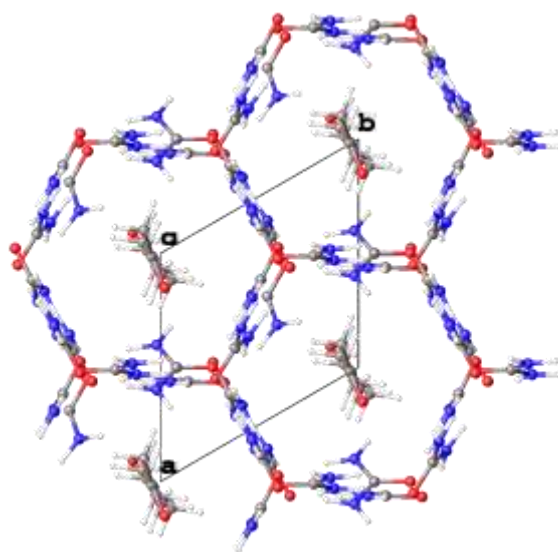
The UIC of 1,6-dibromohexane stands out among UICs in general, as the guest has a commensurate relationship with the host network, despite having no hydrogen bonds between the guest and host. Within the channels, the 1,6-dibromohexane molecules are oriented in a gauche confirmation,<sup>11</sup> overcoming the energy barrier associated with steric hindrance in order to avoid unfavorable Br $\cdots$ Br interactions between guest molecules. This conformation has a significant effect on the host structure, seen in Figure 7, as the channels are distorted relative to those seen in HEX, in order to accommodate the bromo substituents. This results in a monoclinic structure (Table 1).

## Urea 2,7-octanedione

The 2,7-octanedione UIC was first reported by Hollingsworth and co-workers in 1996.<sup>26</sup> Like 1,6-dibromohexane, the 2,7-octanedione guest has a commensurate relationship with the urea network (Figure 8). The presence of the ketone functionalities contributes to hydrogen bonding between the guest and host, facilitated by the twisting of certain urea molecules

away from the plane created by the channel walls. For a unit cell similar in size to that of the hexadecane UIC, this would break the hexagonal symmetry of the structure, but the periodicity of the twisted urea molecules is such that a  $P6_522$  space group is maintained, with an unusually long  $c$  axis of  $76.3\text{\AA}$  as a result, incorporating 3.5 crystallographically independent urea molecules.<sup>27</sup> This provides a unique challenge for structure determination by neutron diffraction that was addressed by using an incident wavelength of  $1.4547\text{ \AA}$  (Table 1). Figure 9 shows how urea molecules in the host walls break from the extended hydrogen bonding network to interact with the carbonyl oxygen of the guest. A hydrogen bond is formed by both NH groups of the molecule with guests in the channels either side, effectively creating a bridge between adjacent channels which is not present in the other UIC examples given here.

---



---

Figure 8. View down  $c$  axis of 2,7-octanedione UIC with unit cell superimposed.  $P6_522$   $a, b = 8.1266(6), c = 76.297(6)$ .

This motif which involves hydrogen bonding between the host and guest is seen for other guest compounds,<sup>26</sup> which have hydrogen bonding acceptor capability, and represents an alternate type of distortion from the conventional HEX type structure than is seen in DBH

and other examples. Instead of a larger-scale supramolecular distortion which alters the channel shape, discrete urea molecules are tilted away from the larger network, bonding with the guest molecule and facilitating commensurate inclusion (Figure 9).

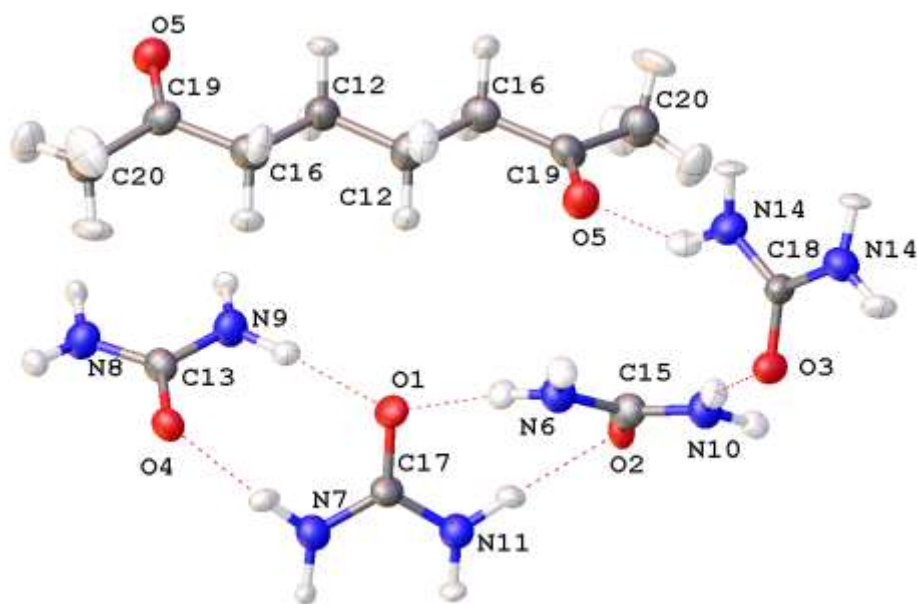


Figure 9. Hydrogen bonding between host and guest in OCT.

#### Urea – DMF co-crystal

Urea and DMF co-crystallize in a 3:1 ratio, not as a typical  $\beta$ -phase channel inclusion compound but as a stoichiometric co-crystal, first reported by Fernandes et al. in 2007.<sup>14</sup> DMF does not meet the requirements of a potential UIC guest as it is too branched and does not contain a long aliphatic chain. The DMF carbonyl oxygen forms a hydrogen bond with two neighboring urea molecules with H...O distances of 1.907(4) and 1.966(3) Å at 30 K. The unit cell of UDM displays a hydrogen bonding pattern between the urea molecules which is similar to that in HEX and other UICs. In effect, the structure comprises small sections of a UIC –type bonded urea network which are ‘interrupted’ by the DMF carbonyl oxygen atom. The packing and bonding of UDM can be seen in



Figure 10, and is discussed further below.

---

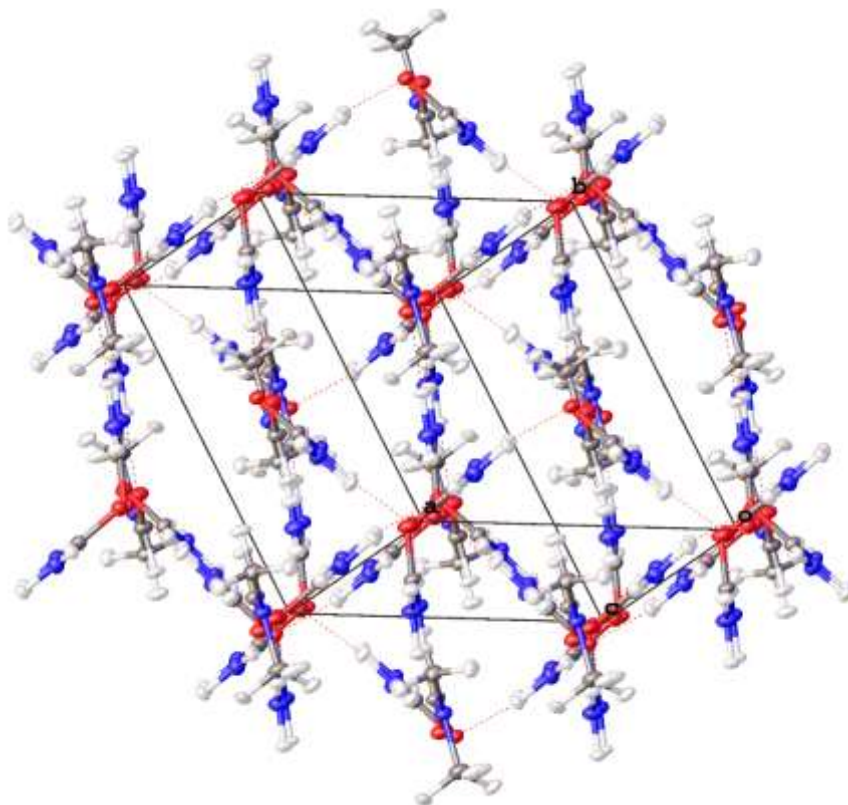


Figure 10. Pseudo-hexagonal packing of UDM, with unit cell superimposed.

#### High pressure studies

In order to ascertain whether the application of high pressure could result in a lowering of the symmetry of the UIC systems as a result of increasing the significance of the guest host interactions, the UICs HEX, DBH, OCT and the co-crystal UDM were studied under high pressure using a diamond anvil cell.<sup>17, 28, 29</sup> HEX, DBH and UDM displayed the conventional compression in unit cell axes and volume which occurs on application of pressure. Crystals of OCT were not resilient to applied pressure, and only one unit cell was collected at 0.71 kbar. Pressures and the associated unit cells are given in

Table 2. Above these pressures, the crystals degraded to the point where single crystal diffraction was no longer possible.

Table 2. Unit cells collected at high pressure

	Pressure/ kbar	$a/\text{\AA}$	$b/\text{\AA}$	$c/\text{\AA}$	$V/\text{\AA}^3$
HEX	Ambient (150 K)	8.1529(5)	8.1529(5)	10.9819(6)	632.2(1)
	2.44	8.190(3)	8.190(3)	10.996(4)	638.7(4)
	5.17	8.116(3)	8.116(3)	10.944(4)	624.3(4)
DBH	Ambient (120 K)	8.5793(6)	10.8922(8)	13.4160(12)	1252.2(2)
	0.50	8.624(2)	10.935(2)	13.664(3)	1287.5(5)
	2.14	8.597(2)	10.872(2)	13.416(3)	1252.4(4)
OCT	Ambient (30 K)	8.1007(5)	8.1007(5)	76.213(5)	4331.1(5)
	0.71	8.115(10)	8.115(10)	76.04(9)	4336(9)
UDM	Ambient (30 K)	7.3797(2)	9.9588(3)	10.9509(2)	671.68(3)
	0.32	7.76(3)	9.829(7)	10.712(10)	710(3)
	4.87	7.621(11)	9.836(11)	10.691(11)	695.9(14)

It is worth noting that the volumes listed in

Table 2 are larger than those seen in the neutron data reported here, as all high pressure diffraction data was collected at ambient temperature.

From the data given in

Table 2, we can see that HEX, DBH and UDM undergo a compression of 2.3, 2.7 and 2.0% for a pressure change of 2.73, 1.64 and 4.55 kbar, respectively. UDM appears to be the least compressible of the structures, despite having the marginally largest void space of the systems studied. All of the structures have similar occupied space percentages, shown in Table 3, calculated using the default settings for void space calculation of OLEX2; resolution 0.2 Å, distance 0.0 Å.<sup>16</sup> None of the structures exhibited any pressure-induced phase changes.

Table 3. Occupied space for all structures.

Structure	Occupied space ambient pressure/ %	Unit cell compression/ %
HEX 150 K	65.1	2.3
DBH 120 K	67.6	2.7
OCT 30 K	64.6	-
UDM 120 K	62.6	2.0

## Discussion

### Crystallization of urea/2,7-octanedione

Initial crystallisation attempts to obtain large crystals of OCT suitable for neutron diffraction were carried out by slow cooling. A ratio of 1:6 urea: 2,7-octanedione was used, in a concentrated MeOH solution at 60°C. The vial containing the solution was placed in a covered Dewar flask surrounded by water at 60°C. The crystals obtained were orange in color (likely as a result of trace impurities), and consistently multiply twinned, although their hexagonal habit was still in evidence (Figure 11). Interestingly, the crystals often break in an unusual way, with an edge portion of one or more hexagonal face of the crystal coming away when agitated suggesting an ‘onion skin’ type of multiple crystal.

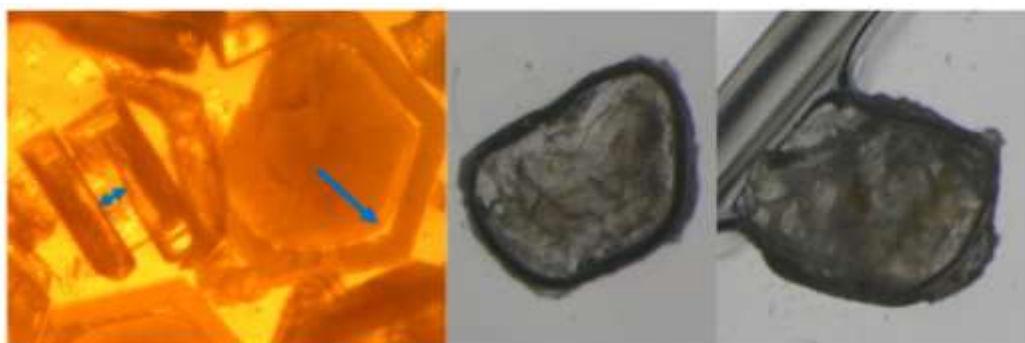


Figure 11. (Left) Crystals from initial crystallisation attempts of OCT. The arrows indicate where the crystal layers are separating. (Right) Crystals obtained using the TEC.

When a suitably large single crystal of OCT was obtained, data were collected with both X-ray and neutron diffraction methods. A structure solution could be obtained from the X-ray data, albeit with poor refinement indicators. Neutron data collected on a large crystal from the initial crystallization attempts at SXD at ISIS, Didcot, UK gave a very poor refinement

against the model obtained from X-ray diffraction. A dual refinement was attempted, fixing the non-hydrogen atom positions obtained from the X-ray model, and then refining against the neutron data to locate hydrogen atoms. However the resulting structure was of low precision. The combination of poor crystal quality and the very large  $c$  unit cell parameter of OCT of 76.3 Å make this a particularly challenging system.

In order to have more precise control over the crystallisation conditions a heating/cooling Peltier thermoelectric cooler (TEC) was designed to allow highly controlled cooling without the apparent multiple crystallization stages suggested by the previously grown samples. A concentrated methanol solution of urea and 2,7-octanedione was cooled from 50°C to 12°C over a period of 4 days and held at 12°C for a further 2 days to optimize crystal size. This resulted in well-formed single crystals of around 8.9 mm<sup>3</sup> volume suitable for single crystal neutron diffraction (see experimental section). Regardless of crystallisation conditions, all OCT crystals showed degradation over time once removed from the mother liquor.

Table 4. Hydrogen bonding data for HEX at 150 K, and DBH, OCT and UDM at 30 K.

	Donor	Hydrogen	Acceptor	D-H/Å	H...A/Å	D...A/Å	D-H...A/°
HEX150	N2	H2A	O1	1.010(4)	1.965(4)	2.9460(19)	163.0(4)
	N2	H2B	O1	1.006(4)	2.009(4)	3.0096(16)	172.5(5)
DBH30	N3	H3A	O8	1.0123(17)	1.9829(19)	2.9934(9)	175.85(18)
	N3	H3B	O10	1.0095(17)	2.0319(19)	2.9991(10)	159.67(16)
	N4	H4A	O10	1.0130(17)	1.9648(18)	2.9704(9)	171.49(17)
	N4	H4B	O8	1.0138(17)	1.9321(18)	2.9227(9)	164.83(15)
	N6	H6A	O2	1.0108(17)	1.9564(18)	2.9580(9)	170.49(17)
	N6	H6B	O10	1.0117(18)	1.9586(19)	2.9395(10)	162.56(15)
	N7	H7A	O10	1.0091(17)	1.9747(19)	2.9740(9)	170.17(18)
	N7	H7B	O2	1.0159(18)	1.979(2)	2.9632(10)	162.28(16)
	N11	H11A	O2	1.0123(16)	1.9850(18)	2.9864(9)	169.69(16)
	N11	H11B	O2	1.0071(18)	2.0145(19)	2.9928(10)	163.19(15)
	N12	H12A	O8	1.0106(16)	1.9894(18)	2.9893(9)	169.75(17)
	N12	H12B	O8	1.0101(17)	1.9321(19)	2.9183(9)	164.61(16)
OCT30	N6	H6A	O1	1.003(19)	1.923(18)	2.918(9)	171.6(15)
	N6	H6B	O4	0.997(14)	1.920(14)	2.879(9)	160.3(13)

UDM30	N7	H7A	O4	0.99(2)	1.972(18)	2.952(9)	170.7(14)
	N7	H7B	O1	0.990(17)	2.031(15)	2.953(9)	154.3(11)
	N8	H8A	O3	0.973(18)	2.052(16)	3.016(7)	170.6(14)
	N8	H8B	O2	0.982(17)	1.929(15)	2.894(9)	167.2(11)
	N9	H9A	O1	0.989(19)	1.949(18)	2.936(9)	175.1(13)
	N9	H9B	O1	0.998(15)	2.003(14)	2.937(9)	154.7(11)
	N10	H10A	O2	0.98(2)	1.963(18)	2.939(9)	175.5(12)
	N10	H10B	O3	0.998(13)	1.973(12)	2.938(7)	161.9(11)
	N11	H11A	O2	1.001(19)	2.031(17)	3.018(9)	168.4(14)
	N11	H11B	O4	1.000(15)	1.897(15)	2.890(9)	171.2(14)
	N14	H14A	O5	0.98(2)	2.10(2)	2.969(10)	146.2(14)
	N14	H14B	O2	1.007(15)	1.971(15)	2.939(9)	160.5(14)
	N4	H4A	O2	1.010(3)	1.893(3)	2.8957(18)	171.5(3)
	N4	H4B	O1	1.009(3)	1.891(3)	2.8334(17)	154.2(3)
	N5	H5A	O3	1.009(3)	1.919(3)	2.9195(17)	170.5(3)
	N5	H5B	O2	1.010(3)	2.290(4)	3.1255(18)	139.2(3)
	N6	H6A	O3	1.009(3)	1.917(3)	2.9088(18)	166.9(3)
	N6	H6B	O1	1.003(3)	2.231(4)	3.0567(18)	138.7(3)
	N7	H7A	O2	1.005(3)	1.883(3)	2.8746(18)	168.5(3)
	N7	H7B	O9	1.000(3)	1.966(3)	2.9634(19)	175.4(3)
	N12	H12A	O9	1.014(3)	1.907(4)	2.921(2)	178.3(3)
	N12	H12B	O2	1.000(3)	1.966(4)	2.8990(18)	154.2(3)
	N13	H13A	O1	1.011(3)	1.869(3)	2.8755(17)	173.1(3)
	N13	H13B	O1	1.004(3)	1.973(4)	2.8785(18)	148.7(3)

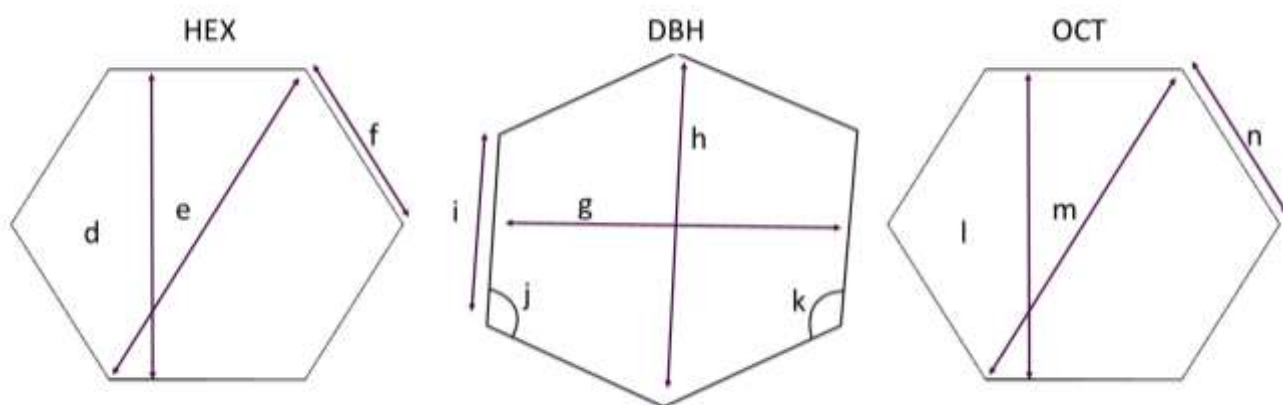


Figure 12. Diagrammatic representations of channel cross-sections and associated lengths/angles for the UIC series (left to right) with guests hexadecane, 1,6-dibromohexane and 2,7-octanedione.

Table 5. Parameters of hexagonal cross-section for each UIC.

HEX 150 K	DBH 30 K	OCT 30 K
$d = 8.15 \text{ \AA}$ $e = 9.41 \text{ \AA}$ $f = 4.71 \text{ \AA}$ $\text{area} = 57.64 \text{ \AA}^2$	$g = 8.58 \text{ \AA}$ $h = 9.97 \text{ \AA}$ $i = 4.98 \text{ \AA}$ $j = 117.4^\circ$ $k = 122.6^\circ$ $\text{area} = 64.43 \text{ \AA}^2$	$l = 8.10 \text{ \AA}$ $m = 9.35 \text{ \AA}$ $n = 4.68 \text{ \AA}$ $\text{area} = 56.90 \text{ \AA}^2$

The values given in Figure 12 and Table 5 show the variation in channel structure between UICs of different guest compounds, DBH in particular stands out, with a larger channel size than its higher symmetry counter-parts. The diameter of the channels in HEX and OCT are similar at 8.15 and 8.10 Å, respectively, whereas DBH has a channel diameter of 8.58 Å. The length of one ‘edge’ of the DBH channel is also larger, at 4.98 Å compared to 4.71 for HEX and 4.68 for OCT. The channels show a reasonable progression in size relative to the size and shape of the guest molecules – hexadecane has the smallest van der Waals radius, followed by 2,7-octanedione and then the significantly larger 1,6-dibromohexane. However, there is no significant change in the average hydrogen bond lengths and distances between the examples (Table 6).

Table 6. Average hydrogen bond parameters for HEX, DBH, OCT and UDM.

	Temperature/K	D-H/Å	H···A/Å	D···A/Å	D-H···A/°
HEX	150	1.01	1.99	2.978	167.8
HEX	260	1.00	1.98	2.929	163.2
DBH	30	1.01	1.98	2.967	167.1
DBH	120	1.01	1.99	2.982	167.0
DBH	260	1.00	2.01	2.991	166.8
OCT	30	0.99	1.98	2.941	164.9
UDM	30	1.01	1.98	2.929	161.6
UDM	120	1.00	2.00	2.946	161.9

Although there is little difference in the average hydrogen bond distances and angles between HEX and DBH, differences can be seen in individual hydrogen bonds. For DBH, the

hydrogen bond associated with the acute angle of the hexagonal channel, N3-H3B $\cdots$ O10, has the longest D-A distance and narrowest angle, 159.67(16) ° of the hydrogen bonds (Table 4). The neighboring bond on the same angle N4-H4B $\cdots$ O8 has an angle of 164.83(15) °. Conversely, the bonds on the widest corner of the hexagonal channel cross section have larger angles of 175.85(18) and 171.49(17) ° for N3 and N4, respectively. These bond angles fall within the same range as those seen in the highly symmetric HEX structure, however their distribution within the network, relative to the distortion in the channels, shows how the finer aspects of hydrogen bonding in these systems are affected by the guest exerting an internal pressure on the host.

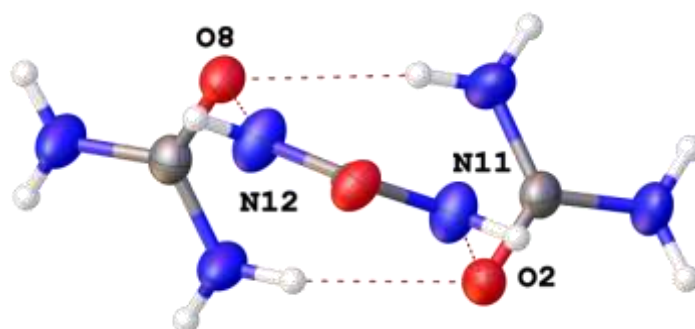
The UIC of (*E,E*)-1,4-diiodo-1,3-butadiene (DIBD) offers an example of host distortion resulting from guest conformation, similar to that seen in DBH.<sup>30</sup> The guest molecule in this instance is planar, the iodine atoms are twisted away from the carbon atom plane by only 1 °. As such, no significant conformational distortions are required in order for DIBD to be accommodated by the urea network, however the host structure is still distorted slightly from the hexagonal symmetry seen in HEX and has the space group  $P2_1/n$ .

The distortion seen in DBH is similar to that of the low temperature phase of the hexadecane analogue,<sup>24</sup> in which the 6<sub>1</sub> screw axis is lost in a hexagonal to orthorhombic transition, as the host lattice is seemingly elongated in one direction. The corner-to-corner distance of HEX goes from 9.41 Å at 150 K to 9.70 Å at 120 K. This is associated with a reduction in the dynamic disorder of the hexadecane guest, albeit not to the extent that it can be modelled. This distortion is more exaggerated in DBH where this distance is 9.97 Å.

Table 6 includes the average hydrogen bond values for all neutron structures collected, including the varied temperatures. Most UICs undergo a temperature dependent phase transition including HEX, as discussed previously.<sup>31</sup> DBH, OCT and UDM do not undergo phase transitions in the temperature ranges discussed here, but DBH has a phase transition at

63°C to a hexagonally symmetric structure phase.<sup>11</sup> The D···A distances of HEX, DBH and UDM tend to be slightly longer at higher temperature, or show no change. HEX seems to be the most susceptible to changes in temperature, with a larger change on average to the D···A bond distances, although this is still only a change of 0.04 Å between 150 and 260 K. The most significant change in an individual bond occurs in DBH where the D···A distance of the hydrogen bond N6-H6B···O1, between two urea molecules, increases by 0.04 Å.

The hydrogen atom positions from the neutron diffraction data show that the N-H bonds in certain locations deviate significantly from the typical planarity of a urea molecule in order to form the motif which creates the walls of the host network. A visual comparison is shown in Figure 13, showing an in-plane view of the hydrogen bonding involving protons H11B and H12B, which are *anti* to the carbonyl group. In the structure determined from X-ray data, the atom positions are assigned according to standard geometries, consistent with the planarity of the urea molecule. Figure 13 however, shows that *anti*-hydrogen atoms are twisted away from the N-C-N plane in order to bond, in this case with oxygen atoms O2 and O8. The same is true for the H3A-N3-C1-N4 torsion angle, at 169.7(2) °.





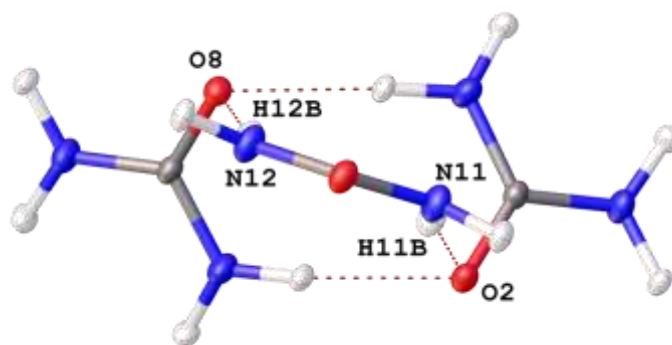


Figure 13. Structure of DBH derived from X-ray data (top) and neutron (bottom) showing the difference in hydrogen atom positions from the two methods.

Table 7. Torsion angles of all bonding hydrogen atoms in DBH at 30 K, using N-C-N to define the plane of the associated urea molecule.

H3A	169.7(2)	H7A	177.5(5)
H3B	5.1(3)	H7B	2.0(1)
H4A	173.4(2)	H11A	171.8(2)
H4B	8.1(2)	H11B	15.1(2)
H6A	178.5(2)	H12A	173.8(2)
H6B	0.3(2)	H12B	3.3(2)

In the tetragonal  $\alpha$ -form of urea, the equivalent torsion angles are  $0^\circ$ , as one would expect from a planar molecule.<sup>32</sup> In the HEX UIC, the equivalent torsional angles are  $176.7(3)$  and  $1.7(3)^\circ$  respectively. Those for urea 1,6-dibromohexane are detailed in Table 7.

The same twisting of urea can be seen in OCT, as the urea bonded with the 2,6-octanedione guest has a greater intramolecular torsion angle than that of neighboring urea molecules. The effect is less than seen for DBH, but a torsional angle of  $11.5(11)^\circ$  is still seen for the urea bonded to the guest molecule (Table 7).

Table 8. Torsion angles of bonding hydrogen atoms in OCT at 30 K.

H6A	178.3(12)	H9A	174.4(11)	H14A	179.2(13)
H6B	7.3(11)	H9B	3.6(16)	H14B	11.5(11)

H7A	177.9(11)	H10A	178.5(11)
H7B	1.4(14)	H10B	2.1(11)
H8A	170.8(12)	H11A	177.7(11)
H8B	3.1(17)	H11B	4.8(14)

Of the hydrogen bonds in OCT, N14-H14A-O5 has the most acute intramolecular bond angle at  $146.2(14)^\circ$ , as the urea molecule twists away from the host walls in order to interact with the guest carbonyl oxygen atom on each side, bridging individual channels.

The urea-DMF hydrogen bonds present in UDM are, on average, of shorter  $D\cdots A$  distance than seen in any of HEX, OCT or DBH, at  $2.929 \text{ \AA}$  (Table 6). Additionally, the angles throughout the structure tend to be more acute. One structural feature present in UDM which is not seen in the UICs is a type of corrugated urea  $\alpha$ -tape, which creates anti-parallel tapes of urea which contribute to the appearance of hexagonal character (Figure 14).

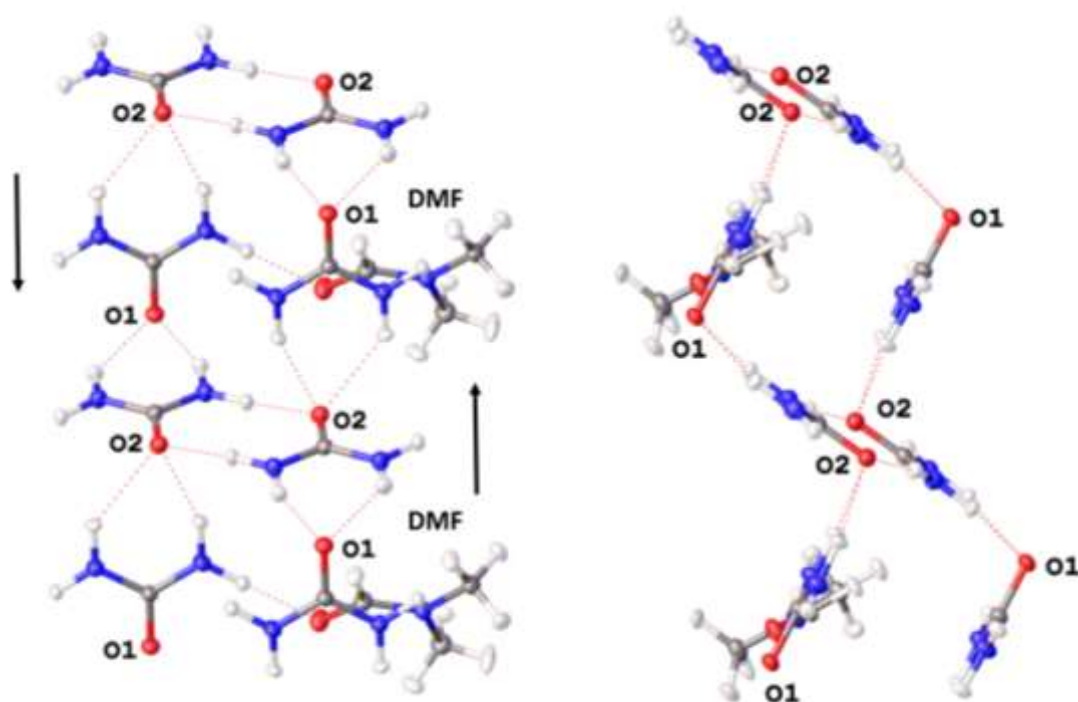


Figure 14. Pseudo  $\alpha$ -urea tape in UDM from two viewpoints.

There is a hydrogen bonding motif present in UDM between two independent urea molecules and DMF. Completed by the inversion center of structure, these create a bonding pattern which closely resembles that found in HEX, forming a portion of the channel walls. In UDM, this section is effectively interrupted by DMF (Figure 15).

Hydrogen bonding data for UDM are shown in Table 4. Figure 15 shows the hydrogen bonding between urea molecules and DMF, which in this structure are closer to being in plane than in the equivalent motif in HEX. The hydrogen bonds to the DMF carbonyl oxygen atom are longer than any urea-urea bonds in the section shown. The bond N12-H13B $\cdots$ O1 has a particularly acute angle of 148.7(3)  $^{\circ}$  compared with the equivalent angle in HEX of 172.5(5)  $^{\circ}$ .

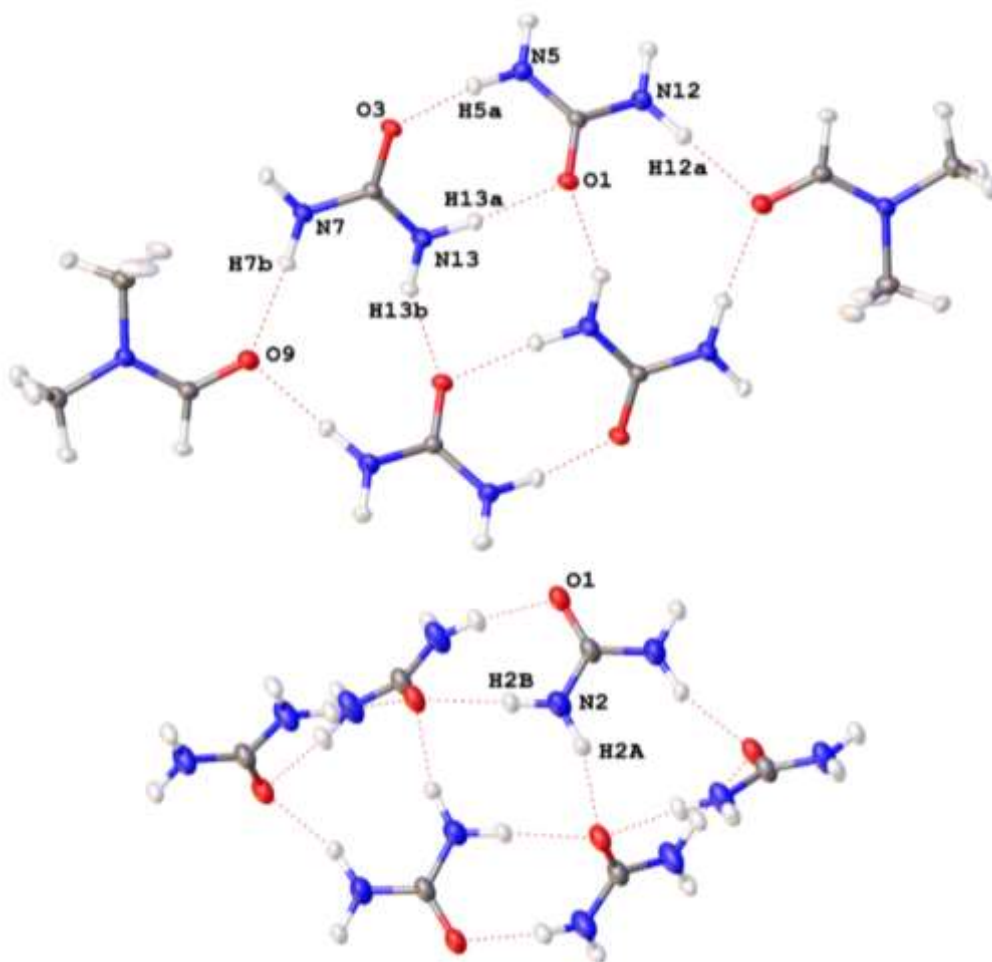


Figure 15. Hydrogen bonding motif in UDM (top) and HEX (bottom).

The UIC of sebaconitrile offers an interesting comparative example of an inclusion compound in which the typical channel structure is disrupted, similar to the effect seen in UDM but in this case maintaining the channel structure of a UIC. In urea/sebaconitrile, segments of the urea host are offset from each other at the junction between adjacent guest molecules.<sup>33</sup> The potential for strong dipole-dipole interactions between adjacent guests would predict a more conventional UIC structure, but the molecules do not fall within van der Waals contact, instead the nitrile groups are hydrogen bonded to two urea molecules in the neighboring channel section, similar to the channel bridging seen in OCT, as the guest bonds with urea host molecules. This sebaconitrile UIC, with space group  $C2/c$ , has similarities with the monoclinic DBH, as hexagonal symmetry is sacrificed in order to accommodate the guest within the channels. Additionally, the channel structure itself is altered significantly compared to HEX, having parallels to the disrupted urea bonding pattern in UDM.

## Conclusions

Perturbations arise in urea inclusion compounds as a result of guest molecule shape, size and bonding capabilities. The size and nature of the guest play a vital role in whether or not an inclusion compound is formed and have a significant influence on the channel structure and host-guest relationship.

Bonding capability influences UIC structure, as guests which are able to form hydrogen bonds may interrupt the urea network and effectively be incorporated into the host structure *via* hydrogen bonding, while still occupying the channel space, resulting in a commensurate host-guest relationship. In the absence of such hydrogen bonding groups, or other particular characteristic, there will be an incommensurate host-guest relationship and the guest position will be unresolved in one dimension.

We have further emphasized the value of neutron diffraction techniques in investigating the nuances of hydrogen bonded systems, as crystal structures determined solely by X-ray diffraction techniques may be missing some of the finer details and subtleties of hydrogen bonded structures. With appropriate techniques neutron quality crystals of even very challenging systems such as OCT can be prepared and studied using modern instrumentation.

Overall, the urea inclusion compound host framework is quite adaptable and significant distortions can be tolerated without significant changes in the hydrogen bond metrics. Distortion of the hexagonal channels can be seen in the shortening and lengthening of hydrogen bonds relative to their position within the network, as seen in DBH, but no significant perturbation from the classic hexagonal channel of HEX is required to accommodate guests of different types. 2,7-octanedione is readily incorporated into a UIC, with a particularly long H $\cdots$ A distance and acute DHA angle relative to bonds in other UICs, highlighting the versatility of the network, and preference for commensurate inclusion when an appropriate guest is present.

## Acknowledgements

We thank Bruker UK Ltd. For funding.

## Notes and references

† Electronic Supplementary Information (ESI) available: CCDC 1504174-1504182 contains the supplementary crystallographic information for this paper.

See DOI: 10.5291/ILL-DATA.5-12-308 and 10.5291/ILL-DATA.5-12-318 for neutron diffraction data.

- (1) Bengen, F.; Schlenk, W. *Cell. Mol. Life Sci.* **1949**, *5*,
- (2) Smith, A. E. *Acta Crystallogr.* **1952**, *5*, 224-235.
- (3) Imashiro, F.; Maeda, T.; Nakai, T.; Saika, A.; Terao, T. *J. Phys. Chem.* **1986**, *90*, 5498-5500.
- (4) Harris, K. D. M.; Smart, S. P.; Hollingsworth, M. D. *J. Chem. Soc., Faraday Trans.* **1991**, *87*, 3423-9.

- (5) Brown, M. E.; Chaney, J. D.; Santarsiero, B. D.; Hollingsworth, M. D. *Chem. Mater.* **1996**, *8*, 1588-1591.
- (6) Forst, R.; Jagodzinski, H.; Boysen, H.; Frey, F. *Acta Crystallogr., Sect. B: Struct. Sci.* **1990**, *46*, 70-78.
- (7) Zerdane, S.; Mariette, C.; McIntyre, G. J.; Lemee-Cailleau, M.-H.; Rabiller, P.; Guerin, L.; Ameline, J. C.; Toudic, B. *Acta Crystallogr., Sect. B: Struct. Sci.* **2015**, *71*, 293-299.
- (8) Chatani, Y.; Taki, Y.; Tadokoro, H. *Acta Crystallogr., Sect. B: Struct. Sci.* **1977**, *33*, 309-311.
- (9) Rennie, A. J. O.; Harris, K. D. M. *P. Roy. Soc. Lond. A Mat.* **1990**, *430*, 615-640.
- (10) Brown, M. E.; Hollingsworth, M. D. *Nature* **1995**, *376*, 323-327.
- (11) Hollingsworth, M. D.; Werner-Zwanziger, U.; Brown, M. E.; Chaney, J. D.; Huffman, J. C.; Harris, K. D. M.; Smart, S. P. *J. Am. Chem. Soc.* **1999**, *121*, 9732-9733.
- (12) Yeo, L.; Harris, K. D. M. *Acta Crystallogr., Sect. B: Struct. Sci.* **1997**, *53*, 822-830.
- (13) Yeo, L.; Harris, K. D. M. *Can. J. Chem.* **1999**, *77*, 2105-2118.
- (14) Fernandes, P.; Florence, A. J.; Fabbiani, F.; David, W. I. F.; Shankland, K. *Acta Crystallogr., Sect. E: Struct. Rep. Online* **2007**, *63*, o4861.
- (15) Sheldrick, G. *Acta Crystallogr., Sect. C: Cryst. Struct. Commun.* **2015**, *71*, 3-8.
- (16) Dolomanov, O. V.; Bourhis, L. J.; Gildea, R. J.; Howard, J. A. K.; Puschmann, H. *J. Appl. Crystallogr.* **2009**, *42*, 339-341.
- (17) Lee, R.; Howard, J. A. K.; Probert, M. R.; Steed, J. W. *Chem. Soc. Rev.* **2014**, *43*, 4300-4311.
- (18) Piermarini, G. J.; Block, S.; Barnett, J. D.; Forman, R. A. *J. Appl. Phys.* **1975**, *46*, 2774-2780.
- (19) Probert, M. R.; Coome, J. A.; Goeta, A. E.; Howard, J. A. K. *Acta Crystallogr., Sect. A: Found. Crystallogr.* **2011**, *67*, C528.
- (20) Probert, M. R.; Robertson, C. M.; Coome, J. A.; Howard, J. A. K.; Michell, B. C.; Goeta, A. E. *J. Appl. Crystallogr.* **2010**, *43*, 1415-1418.
- (21) Schulz, T.; Meindl, K.; Leusser, D.; Stern, D.; Graf, J.; Michaelsen, C.; Ruf, M.; Sheldrick, G. M.; Stalke, D. *J. Appl. Crystallogr.* **2009**, *42*, 885-891.
- (22) Forst, R.; Jagodzinski, H.; Boysen, H.; Frey, F. *Acta Crystallogr., Sect. B: Struct. Sci.* **1987**, *B43*, 187-97.
- (23) Harris, K. D. M. *J. Phys. Chem. Solids* **1992**, *53*, 529-537.
- (24) Yeo, L.; Kariuki, B. M.; Serrano-Gonzalez, H.; Harris, K. D. M. *J. Phys. Chem. B* **1997**, *101*, 9926-9931.
- (25) Fucke, K.; Edwards, A. J.; Probert, M. R.; Tallentire, S. E.; Howard, J. A. K.; Steed, J. W. *ChemPhysChem* **2013**, *14*, 675-679.
- (26) Brown, M. E.; Chaney, J. D.; Santarsiero, B. D.; Hollingsworth, M. D. *Chem. Mater.* **1996**, *8*, 1588-1591.
- (27) Steed, K. M.; Steed, J. W. *Chem. Rev.* **2015**, *115*, 2895-2933.
- (28) Katrusiak, A. *Acta Crystallogr., Sect. A: Found. Crystallogr.* **2008**, *64*, 135-148.
- (29) Boldyreva, E. *Acta Crystallogr., Sect. A: Found. Crystallogr.* **2008**, *64*, 218-231.
- (30) Lashua, A. F.; Smith, T. M.; Hu, H.; Wei, L.; Allis, D. G.; Sponsler, M. B.; Hudson, B. S.; *Cryst. Growth Des.* **2013**, *13*, 3852-3855.
- (31) Harris, K. D. M. *Chem. Soc. Rev.* **1997**, *26*, 279-289.

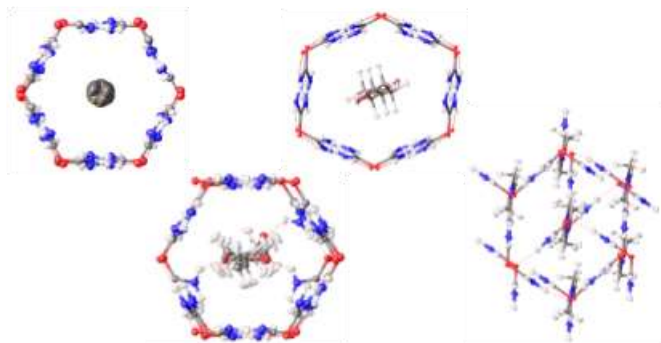
- (32) Swaminathan, S.; Craven, B. M.; McMullan, R. K. *Acta Crystallogr., Sect. B: Struct. Sci. B* **1984**, *40*, 300-306.
- (33) Hollingsworth, M. D.; Santarsiero, B. D.; Harris, K. D. M. *Angew. Chem. Int. Ed.* **1994**, *33*, 649-652.

For Table of Contents Use Only

## Neutron Diffraction Studies on Guest-Induced Distortions in Urea Inclusion Compounds

*Rachael Lee, Sax A. Mason, Estelle Mossou, Glenn Lamming, Michael R. Probert and*

*Jonathan W. Steed*



A systematic study of the bonding in a series of urea inclusion compounds was carried out by neutron diffraction. A simple heating/cooling Peltier thermoelectric cooler was designed for growing large single crystals suitable for neutron diffraction.

Supporting information is available: CCDC codes 1504174 – 1504182 containing crystallographic information for this paper.